

AD-A131 083

ANODE PLASMA EXPANSION IN PINCH-REFLEX DIODES(U) NAVAL  
RESEARCH LAB WASHINGTON DC D G COLOMBANT ET AL.  
16 AUG 83 NRL-MR-5148

1/1

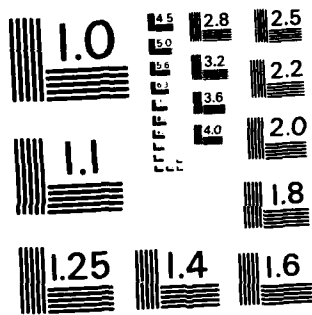
UNCLASSIFIED

F/G 12/1

NL




END  
DATE  
FILMED  
8 83  
DT



MICROCOPY RESOLUTION TEST CHART  
NATIONAL BUREAU OF STANDARDS-1963-A

ADA 131083

SECURITY CLASSIFICATION OF THIS PAGE (When Data Entered)

REPORT DOCUMENTATION PAGE		READ INSTRUCTIONS BEFORE COMPLETING FORM
1. REPORT NUMBER NRL Memorandum Report 5148	2. GOVT ACCESSION NO. AD-4131083	3. RECIPIENT'S CATALOG NUMBER
4. TITLE (and Subtitle) ANODE PLASMA EXPANSION IN PINCH-REFLEX DIODES	5. TYPE OF REPORT & PERIOD COVERED Interim report on a continuing NRL problem.	
	6. PERFORMING ORG. REPORT NUMBER	
7. AUTHOR(s) D.G. Colombant and Shyke A. Goldstein*	8. CONTRACT OR GRANT NUMBER(s)	
9. PERFORMING ORGANIZATION NAME AND ADDRESS Naval Research Laboratory Washington, DC 20375	10. PROGRAM ELEMENT, PROJECT, TASK AREA & WORK UNIT NUMBERS DE-AI08-79DP40092; 47-0879-0-3	
11. CONTROLLING OFFICE NAME AND ADDRESS U.S. Department of Energy Washington, DC 20545	12. REPORT DATE August 16, 1983	
	13. NUMBER OF PAGES 16	
14. MONITORING AGENCY NAME & ADDRESS (if different from Controlling Office)	15. SECURITY CLASS. (of this report) UNCLASSIFIED	
	15a. DECLASSIFICATION/DOWNGRADING SCHEDULE	
16. DISTRIBUTION STATEMENT (of this Report)  Approved for public release; distribution unlimited.		
17. DISTRIBUTION STATEMENT (of the abstract entered in Block 20, if different from Report)		
18. SUPPLEMENTARY NOTES  *Present address: JAYCOR, Inc., Alexandria, VA 22304 This work was supported by the U.S. Department of Energy.		
19. KEY WORDS (Continue on reverse side if necessary and identify by block number) Magnetohydrodynamic Numerical solution Ion diode Ion beam brightness <i>pinch reflex data</i>		
20. ABSTRACT (Continue on reverse side if necessary and identify by block number) Anode plasma expansion in PRD is investigated using a one-dimensional magneto-hydrodynamic model. Early in time, the plasma undergoes thermal expansion and its front is slowed down due to $j \times B$ . After the current has reached its maximum and for small radius where $j$ and $B$ are larger, $j \times B$ may accelerate the bulk of the anode plasma to large velocities. Good qualitative agreement is obtained with the experimental observations of the time dependence of the plasma velocity as well as its radial profile. The maximum expansion velocities reach tens of $\text{cm}/\mu\text{sec}$ . <i>micros</i> .		

DD FORM 1473 JAN 73

EDITION OF 1 NOV 65 IS OBSOLETE  
S/N 0102-014-6601

SECURITY CLASSIFICATION OF THIS PAGE (When Data Entered)

CONTENTS

Introduction ..... 1

Model ..... 3

Results ..... 8

Conclusion ..... 13

Acknowledgments ..... 13

References ..... 14

Accession For		
NTIS GRA&I	<input checked="" type="checkbox"/>	
DTIC TAB	<input type="checkbox"/>	
Unannounced	<input type="checkbox"/>	
Justification		
By _____		
Distribution/ _____		
Availability Codes		
Dist	Avail and/or	
	Special	
<b>A</b>		



PRECEDING PAGE BLANK-NOT FILLED

## ANODE PLASMA EXPANSION IN PINCH-REFLEX DIODES

### Introduction

Anode plasma dynamics is important in all pulsed-power ion diodes. In most diodes, it leads to anode-cathode (A-K) gap closure and to the ion pulse termination. It may also have undesirable effects on ion beam brightness since ions extracted from a non-uniform surface will not be accelerated in the A-K gap for the same amount of time and not necessarily in the same direction. Few studies<sup>1-4</sup>, experimental or theoretical, have been made of this critical phenomenon. One study<sup>4</sup> has determined some experimental characteristics of this expansion. First, large closure velocities up to 30 cm/ $\mu$ sec have been observed. Second, this large expansion is observed only late into the pulse (about 30 nsec into the ion pulse) and finally it takes place preferentially near the anode axis of symmetry. The 30 cm/ $\mu$ sec measured would correspond to a thermal expansion of a 0.4 keV CH<sub>2</sub> plasma which cannot be obtained by ohmic heating alone for the measured plasma parameters. The two main theoretical attempts at explaining the anode plasma expansion have not been very conclusive. Nardi et al<sup>1</sup> have shown that 10 cm/ $\mu$ sec expansion takes place near the anode center because of the electron energy deposition in that region but they did not reproduce the larger velocities observed nor the long delay in the expansion. Prono et al<sup>2</sup> have studied a charge-exchange mechanism to account for the large expansion velocity but this mechanism does not explain the favored central expansion nor the large delay in the expansion. In the present work, we describe a model based on the dominant role played by the ( $j \times B$ ) force in the anode plasma expansion. In particular, the main results from this model are consistent with large final expansion velocities, with large expansion near the anode

Manuscript approved June 20, 1983.

center and with a long delay before fast expansion sets in. First, the model and the assumptions are presented. Then results and discussions of the most influential parameters follow.

## Model

The geometry of the model is shown in Fig. 1. The anode foil is planar and made of a non-conducting material (polyethylene). When electrons from the cathode accumulate on the anode surface, flash-overs occur and an anode plasma is formed just in front of the anode foil. This anode plasma serves as the source of the ions. When ions leave the plasma generating an ion current in the diode, the thermal electrons that are left behind flow radially inwards through the anode plasma where they are collected on a conducting rod at  $r = r_{\min}$ . The rest of the diode current flows from the cathode in the form of a relativistic electron beam (REB) which is assumed to pinch in vacuum from the diode radius  $R$  to a radius comparable to  $r_{\min}$ . For  $z < 0$ , all the diode current is carried in the conducting rod and therefore, the magnetic field due to the total current develops behind the anode plasma. On the other hand, for  $z > 0$ , only a fraction of the total current contributes to the magnetic field. Because of that configuration, a gradient in magnetic pressure develops in the plasma. The force on the plasma due to this gradient is described by the local  $(j \times B)$  where  $j$  is due to the thermal electron current in the anode plasma. Notice that in the present model, the REB does not deposit its energy in the anode plasma but does contribute to the magnetic field there. The anode plasma is collision-dominated and thus a fluid description is used to study its motion in the  $z$ -direction. For simplicity, we have performed one-dimensional studies of the anode plasma motion at various radii, approximating a two-dimensional picture by assuming that the thermal electron current has only a radial component.

The equations which describe the anode plasma are the magnetohydrodynamic equations<sup>5</sup> which express conservation of mass, momentum and energy. A magnetic diffusion equation closes the system. In the momentum equation, both

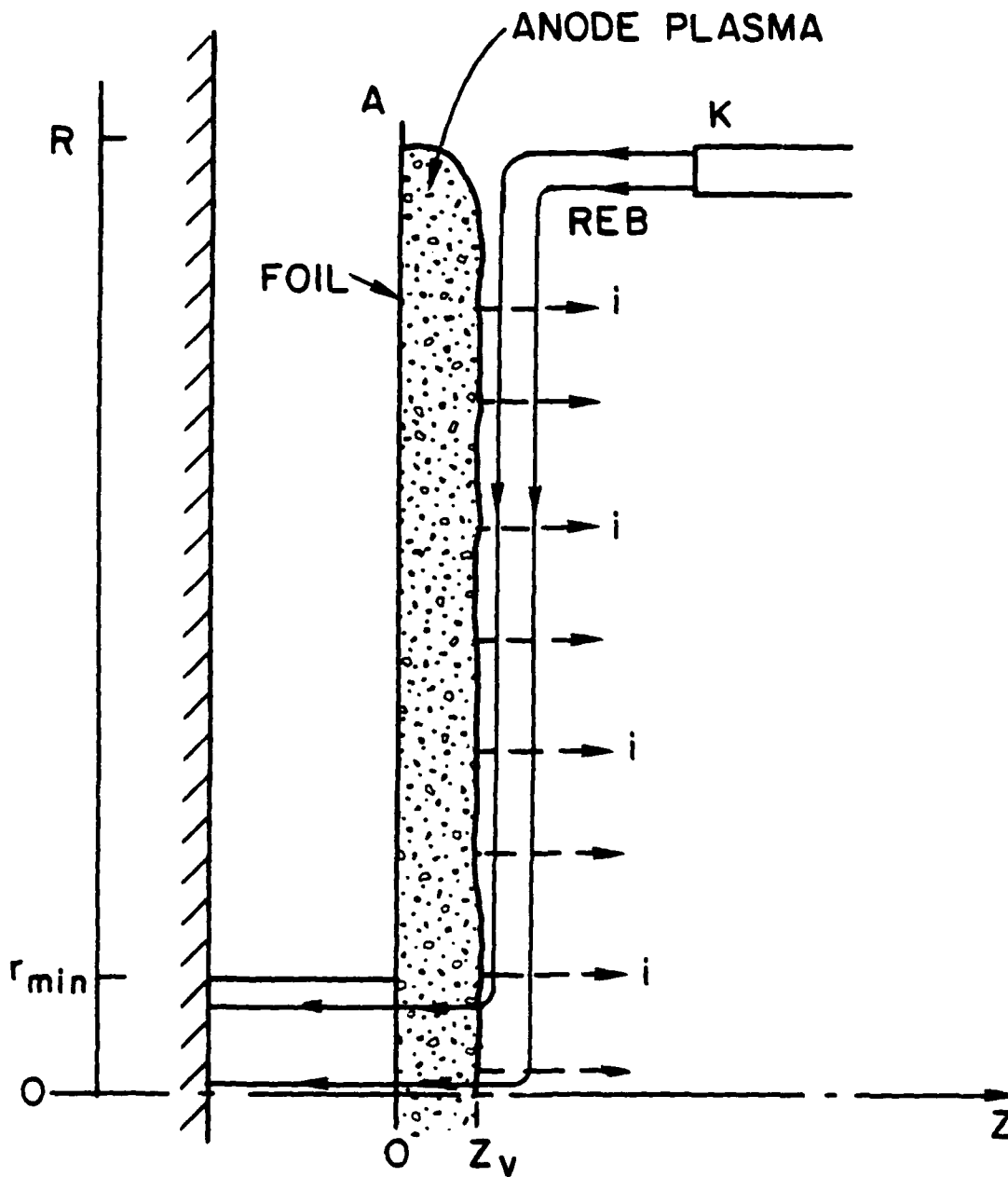


Fig. 1. Schematic of the anode plasma model for pinch-reflex diode-plasma.  
Expansion is studied in the z-direction as a function of radius.

thermal pressure gradient and  $j \times B$  act on the plasma. In the energy equation, radiation losses have been neglected and the energy input into the plasma comes from the Ohmic heating term as well as  $j \times B$  acceleration. The initial and boundary conditions which complete the set of assumptions are as follows. A low temperature is assumed for the  $C_2H_4$  plasma at  $t = 0$  ( $T \approx 0.5$  eV) as well as near-solid density ( $n_1 = n_{\text{solid}}/10$ ) which is assumed uniform over a distance of  $10^{-5}$  cm and corresponds roughly to an energy deposition<sup>6</sup> of  $0.1 \text{ J/cm}^2$ . The electron and ion current waveforms are based on ref. 4. They rise linearly in time in 30 nsec and remain constant thereafter as shown in Fig. 2. As for boundary conditions, the ion current density  $j_z$  for  $z > z_v$  where  $z_v$  denotes the plasma-beam interface is assumed to be inversely proportional to  $r$ . This relationship has been demonstrated both experimentally<sup>7</sup> and in particle simulation<sup>8</sup>. The resulting B field at  $z = z_v$  due to the ion current is independent of radius. The B field due to the REB current is inversely proportional to  $r$  for  $z = 0$  and  $z = z_v$ . Because of the time dependence of the currents (Fig. 2), the B field increases with time both at  $z = 0$  and  $z = z_v$  and is larger at  $z = 0$ . The boundary condition to determine the position of  $z_v$  follows from both plasma expansion and plasma erosion. The expansion is determined simply by the plasma boundary velocity  $v_p(z_v)$ . The anode plasma erosion is due to the ion beam extraction by the diode electric field at  $z > z_v$  which prevents plasma electrons from following the ions. The expression for  $z_v$  is then

$$v_F = \frac{dz_v}{dt} = v_p(z_v) - \frac{j_1}{n_1}$$

where the subscript  $i$  refers to the ions. From that expression, and for typical peak parameters:  $j_1 = 100 \text{ kA/cm}^2$ ,  $v_p = 10^7 \text{ cm/sec}$ , the plasma number

density at  $z_v$  is  $n_i \approx 10^{17} \text{ cm}^{-3}$  or  $\rho \approx 10^{-6} \text{ g/cm}^3$  for a  $\text{CH}_2$  plasma.

Other features of the model concern its treatment of the equation of state and of the electrical resistivity. The equation of state for  $\text{CH}_2$  was taken from standard SESAME tables except that at low temperatures and high density, corrections were made to take into account the fact that  $\text{C}_2\text{H}_4$  dissociated into  $\text{CH}_2$ , then into  $\text{C} + \text{H} + \text{H}$ . Electrical resistivity was assumed to be classical and was supplemented by electron-neutral collision resistivity at low temperatures and by anomalous resistivity at high temperature and low density.

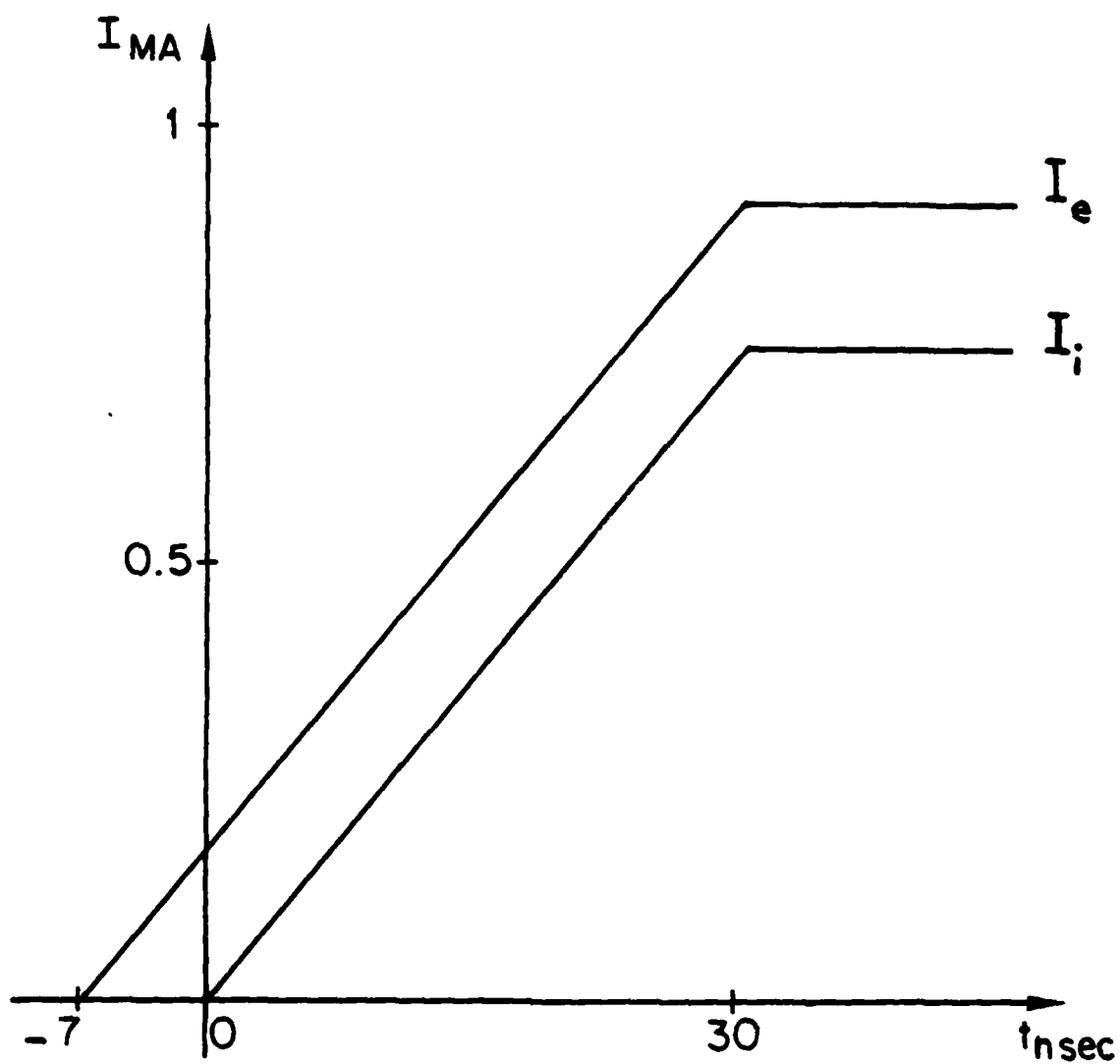


Fig. 2. Ion and electron current waveforms - note delay in ion current rise.

## Results

Results were obtained for  $I_{i\max} = I_{e\max} = 50$  kA,  $\tau_p$  (linear ramp) = 30 nsec (see Fig. 2),  $R = 5$  cm and initial plasma mass density/unit area =  $3.5 \times 10^{-6}$  g/cm<sup>2</sup>. Plasma expansion was calculated for the different radii  $r = 1, 2.5$  and  $4$  cm. The following is a brief summary and analysis of the results. In all cases, pressure gradients dominated the  $j \times B$  force in the first few nanoseconds and gave rise to expansion velocities of a few times the thermal sound speed or a few cm/ $\mu$ sec.

When the  $j \times B$  force becomes important, it first has the effect of slowing down the plasma in the vicinity of  $z_v$ . In order to explain that effect, we use as an example the information in Fig. 3 where density, velocity, B-field and current density profiles are shown as a function of  $z$  at  $t = 14$  nsec and  $r = 2.5$  cm. The main feature of the B-field profile in Fig. 3a is the dip inside the plasma. Because  $j_r = -\frac{c}{4\pi} \frac{\partial B}{\partial z}$ , we see that for  $z < z_d$ , ( $j \times B$ ) accelerates the plasma outwards whereas for  $z > z_d$ , ( $j \times B$ ) slows down the plasma. The reasons for this dip are the following: near  $z = 0$ , the plasma density is very high, the temperature rises very slowly and the magnetic field diffuses rapidly through the plasma as shown by the B-field plateau. For  $z \lesssim z_v$  on the other hand, the plasma density is low, its temperature is high and it expands in the axial direction. This expansion reduces the magnetic field inside the plasma, slowing down the diffusion process which is already weaker than on the low-temperature side (at  $z \approx 0$ ). The ensuing confinement effect for  $z_d < z < z_v$  is seen on the velocity and density profiles in Fig. 3c,d. The density profile in Fig. 3d stays nearly a constant due to the  $j \times B$  slowing down effect in the above domain. When the  $j \times B$  force was artificially suppressed in the calculations, no density plateau was observed.

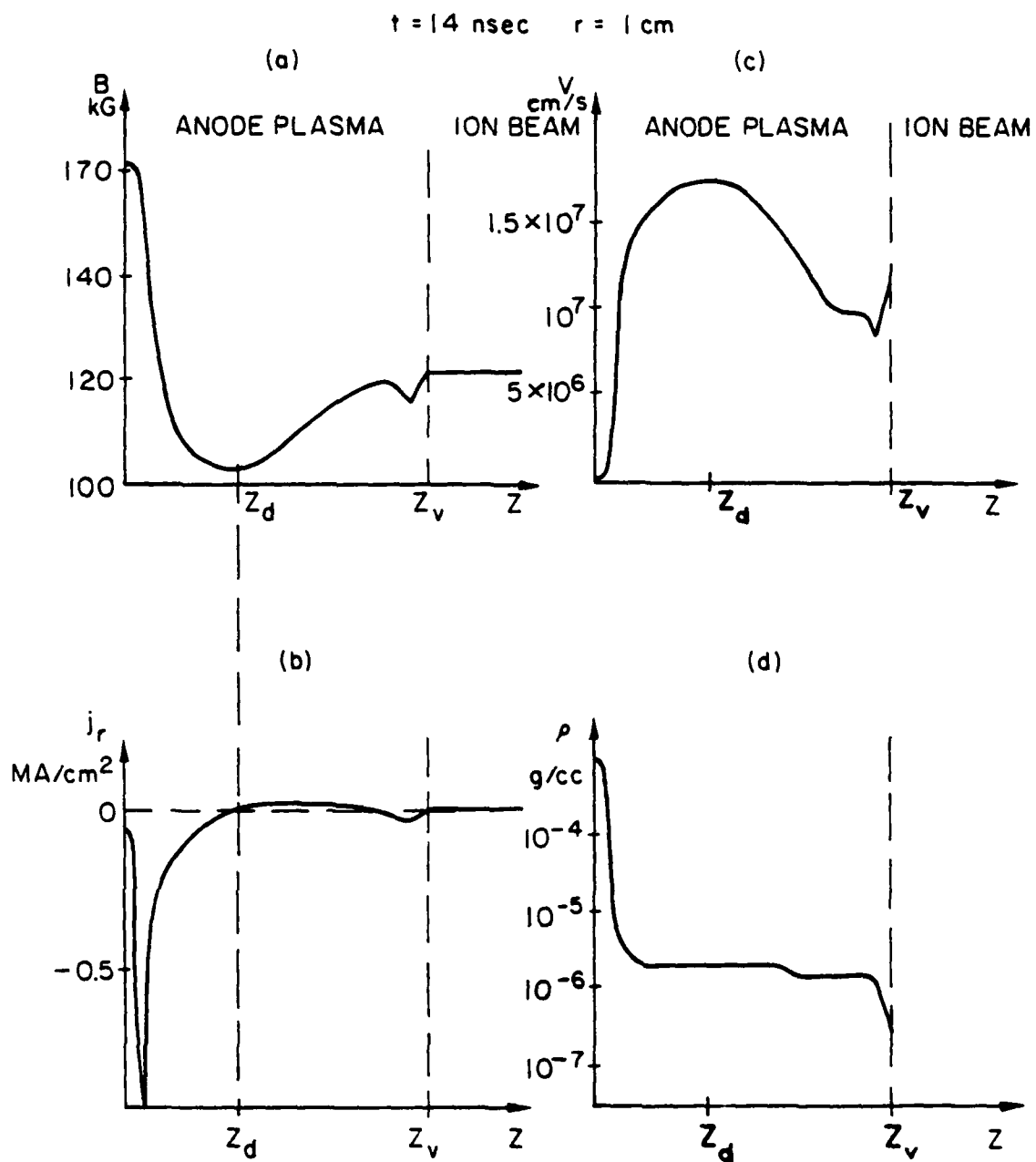


Fig. 3. Typical B-field, plasma current density, axial velocity and mass density profiles as a function of distance along axis. Note that the origin in  $z$  corresponds to the cathode side of the anode foil. Profiles are shown at  $t = 14 \text{ nsec}$  for  $r = 1 \text{ cm}$ .

As time increases,  $j \times B$  may be large enough so that the velocity profile between  $z_d$  (higher velocity) and  $z_v$  (lower velocity) changes significantly. In that case, the distance  $(z_v - z_d)$  will shrink to 0 during the ion beam pulse duration. The front velocity  $v_F$  will then exhibit a sudden change in value from  $v(z_v)$  to  $v(z_d)$  as  $(z_v - z_d)$  goes to zero. The whole anode plasma at  $z \leq z_d$  is accelerated during that time, reaching velocities of tens of cm/ $\mu$ sec. This situation occurs especially at small radii where both  $j$  and  $B$  are larger. For the case of Fig. 3, the velocity  $v_p(z_d)$  remains approximately constant at 16 cm/ $\mu$ sec from 10 to 30 nsec whereas  $v_p(z_v)$  gradually decreases from 12 cm/ $\mu$ sec to 5 cm/ $\mu$ sec. Later in the pulse, as  $(z_v - z_d)$  approaches zero, the plasma moves at velocities up to 30 cm/ $\mu$ sec at  $t = 50$  nsec. At large radii however,  $j \times B$  is smaller and does not generate a velocity differential between  $z_d$  and  $z_v$  large enough to cause complete shrinkage of this gap. The plasma front velocity  $v_F$  is nearly equal to 10 cm/ $\mu$ sec and does not undergo any abrupt changes. The plasma front location as a function of radius is shown in Fig. 4 at various times. We see that the experimental observations of large velocities late in the pulse as well as larger acceleration near the anode center are all in qualitative agreement with the results of the present model. The results of the present model have been checked for their sensitivity to the following variations.

Initial plasma mass: the mass was changed from  $3.5 \times 10^{-6}$  g/cm<sup>2</sup> to  $8.5 \times 10^{-6}$  g/cm<sup>2</sup> for  $r = 1$  cm while keeping the same initial density gradient. The thermal expansion in the early stages is very similar and resulted in the same value for the front velocity. Then, in both cases, the current density peaks at the foot of the density gradient and gradually erodes it. In time, this plasma expands and as mentioned previously is slowed down by the  $j \times B$  force. Up to times of 30 nsec, there are no major differences between the two mass

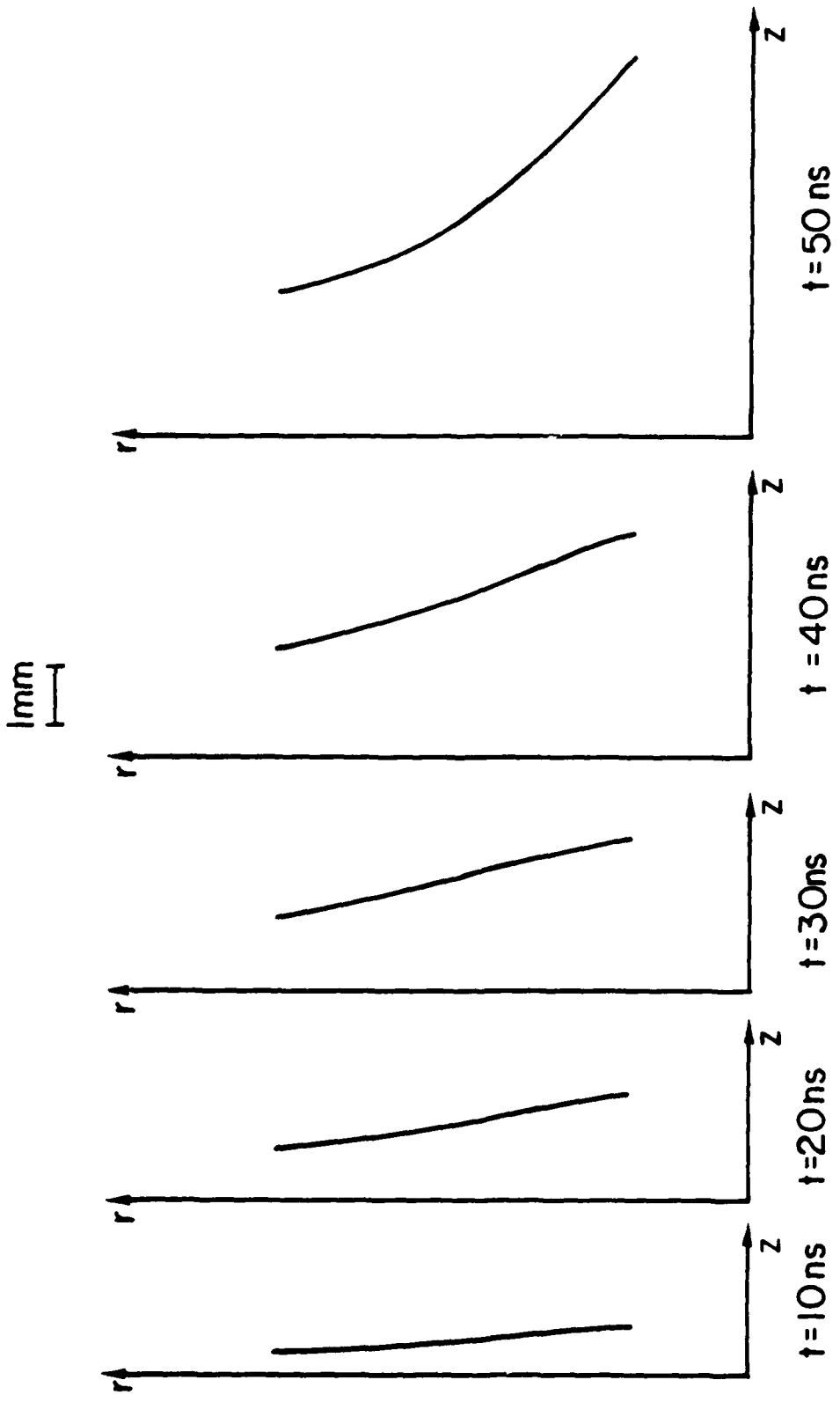


Fig. 4. Position of the anode plasma front (defined by  $z_v$ ) as a function of time. Calculations have been made at three different radii.

density cases. However, later in the pulse, the reduction in density near  $z = 0$  for the more massive target is slower and once the plasma starts to be accelerated from the back, it reaches lower velocities since there is more of it. An integral of the momentum equation gives the average velocity in the later stages when the total pressure differential across the plasma can be neglected

$$\langle v \rangle = \frac{I^2}{200 \pi m_0 r^2} t_{\text{acc}}$$

where  $t_{\text{acc}}$  is the time over which acceleration from the back takes place. This equation gives also a very rough check on the code (because of the assumption on the pressure differential). For example, for the case of Fig. 3, we find that for  $I \approx 1.5$  MA,  $t_{\text{acc}} = 25$  nsec,  $r = 1$  cm and  $m_0 = 3.5 \cdot 10^{-6}$  g/cm<sup>2</sup>, then  $\langle v \rangle = 26$  cm/ $\mu$ sec whereas the code gives 23 cm/ $\mu$ sec at  $t = 50$  nsec. For  $m_0 = 8.5 \times 10^{-6}$  g/cm<sup>2</sup>, the observed pressure differential is not negligible and we find that  $\langle v \rangle = 10.7$  cm/ $\mu$ sec whereas the code gives 15 cm/ $\mu$ sec at  $t = 50$  nsec.

Maximum temperature in the low-density plasma: a low-density plasma ( $\rho \lesssim 10^{-7}$  g/cm<sup>3</sup>) may be present in the calculations at both boundaries, on the cathode side naturally and on the anode side late in the pulse when the whole plasma is being pushed from behind by the ( $j \times B$ ) force. If current is still allowed to flow in this region, the temperature can reach several keV. Because of the low plasma density ( $n_e \approx 10^{15}$  cm<sup>-3</sup>) and the high current density ( $j \approx 10^6$  A/cm<sup>2</sup>, see Fig. 3b) the drift velocity ( $\bar{v}_D \sim 5 \times 10^9$  cm/sec) exceeds the thermal velocity for the electrons and the plasma becomes anomalously resistive. In order to avoid such excessive heating, a simple anomalous resistivity model was used and a temperature limit was also imposed

in that region. The present results were obtained for  $T \leq 200$  eV. This limit affects only the results for the lower mass-density case at  $r = 1$  cm. For all the other cases, the temperature did not reach 100 eV in that region (either because of the larger mass or the lower current).

### Conclusion

In conclusion, it has been shown for the first time that anode plasma expansion can be explained in terms of a magneto-hydrodynamic model and that the main observations of the time history of the expansion, large final velocities (30 cm/ $\mu$ sec) and preferred acceleration near the anode center are well reproduced by the model. Improvements to the present model should include a detailed treatment of the resistivity in the low-density regions ( $n_e < 10^{15}$  cm $^{-3}$ ) as well as a two-temperature model. The important implication of this work for plasma diodes is that there is a limit on how small high power diodes can be made and how short the pulse length should be before running into limitations due to anode plasma expansion. Other diodes besides the Pinch-Reflex diode should also be investigated in that respect using models similar to that one presented here.

### Acknowledgments

This work was supported by the U.S. Department of Energy.

### References

1. E. Nardi, E. Peleg and Z. Zinamon, *Plasma Physics* 20, 597 (1978).
2. D. S. Prono, H. Ishizuka, E. P. Lee, B. W. Stallard and W. C. Turner, *J. Appl. Phys.* 52, 3004 (1981).
3. S. A. Goldstein, D. W. Swain, G. R. Hadley and L. P. Mix, *International Topical Conference in Electron Beam Research & Technology*, Albuquerque, 1975, p. 262.
4. J. W. Maenchen, F. C. Young, R. Stringfield, S. J. Stephanakis, D. Mosher, Shyke A. Goldstein, R. D. Guenario and G. Cooperstein, to be published in *J. Appl. Phys.*
5. S. I. Braginskii, in Reviews of Plasma Physics, Vol. I, edited by M. A. Leontovich (Consultants Bureau, New York, 1965), p. 262
6. S. Humphries Jr., *Nucl. Fusion* 20, 1549 (1980).
7. A. E. Blaugrund, S. J. Stephanakis and Shyke A. Goldstein, *J. Appl. Phys.* 53, 7280 (1982).
8. A. T. Drobot, R. J. Barker, R. Lee, A. Sternlieb, D. Mosher and Shyke A. Goldstein, *Proceedings of the 3rd International conference on High Power Electron and Ion Beam Research and Technology*, Novosibirsk, July 1979, p.647.

LATE  
LME